

Chapter

Overview of Existing and Future Advanced Satellite Systems

John Nguyen

Abstract

This chapter presents an overview of legacy, existing, and future advanced satellite systems for future wireless communications. The overview uses top-down approach, starting with a comparison between a typical commercial regular satellite system and a high-throughput satellite (HTS) system, following by a discussion on commonly used satellite network topologies. A discussion on the design of satellite payload architectures supporting both typical regular satellite and HTS with associated network topologies will be presented. Four satellite payload architectures will be discussed, including legacy analog bent-pipe satellite (ABPS); existing digital bent-pipe satellite (DBPS) and advanced digital bent-pipe satellite using digital channelizer and beamformer (AdDBPS-DCB); and future advanced regenerative on-board processing satellite (AR-OBPS) payload architectures. Additionally, various satellite system architectures using AdBP-DCBS and AR-OBPS payloads for the fifth-generation (5G) cellular phone applications will also be presented.

Keywords: high-throughput satellite, analog bent-pipe satellite, digital bent-pipe satellite, digital channelizer and beamformer, advanced regenerative on-board processing satellite, cellular phone

1. Background and introduction

Recently, the space industry has pointed out that in the past 5 years, the commercial market has been driving the advancement of satellite technology. Lockheed Martin is building commercial satellites (e.g., Hellas-sat series) with advanced on-board processing capabilities for the Saudi Arabian [1]. Hellas satellites probably will be the first commercial HTS with a very advanced digital processor on-board. The focus of this chapter will be on commercial satellite systems for communication applications, and a comparison study between commercial HTS and typical satellites systems conducted by Inmarsat will be provided [2].

For communication applications, commercial satellite systems have been categorized as mobile satellite services (MSSs), fixed satellite services (FSSs), broadcast satellite services (BSSs), and high-throughput satellite (HTS) services. Depending on the services, satellite payload architecture will be designed to meet the specified requirements for that service. Basically, satellite payload architecture can be classified into four categories: (1) analog bent-pipe satellite (ABPS); (2) digital bent-pipe satellite (DBPS); (3) advanced digital bent-pipe satellite using digital channelizer and beamformer (AdDBPS-DCB); and (4) advanced regenerative on-board processing satellite (AR-OBPS). This chapter provides an overview of these payload

architectures and presents two satellite system architectures using AdBPS-DCBS and AR-OBPS payloads for the fifth-generation cellular phone (5G) applications.

The chapter is organized as follows: Section 2 provides a comparison between commercial HTS and typical satellite systems; Section 3 discusses the typical satellite network topologies; Section 4 presents an overview of legacy ADPS transponder, existing DBPS transponder, AdBPS-DCBS transponder, and AR-OBPS satellite system; Section 5 discusses the use of AdBPS-DCBS transponder and AR-OBPS payloads for the fifth-generation cellular phone (5G) applications; and Section 6 concludes the chapter with a summary and brief discussion of way forward.

2. Typical commercial satellites and HTS comparison

Typical and regular commercial satellites are operating in C-band, Ku-band, and Ka-band with downlink frequencies approximately at 4, 12, and 40 GHz, respectively. For C-band, Ku-band, and Ka-band, the spectrum bandwidths available by geostationary orbital position are 500 MHz, 500 MHz, and 3.5 GHz, respectively. Typical antenna types for these regular commercial satellites are pointed antenna type with a single beam. Typical diameters for these pointed antennas are (a) greater than 1.8 m for C-band; (b) 0.9–1.2 m for Ku-band; and (c) 0.6–1.2 m for Ka-band satellite. **Figure 1(a)** illustrates a typical regular commercial satellite.

Typical HTSs are usually also operating in Ku-band and Ka-band with the same downlink frequencies as the regular satellites except that they employ multiple pointed beam as oppose to a single-pointed beam. **Figure 1(b)** describes a multiple beam HTS system. The salient feature of multiple beams is the frequency reuse. The frequency reuse is defined as the number of times a satellite can reuse the same spectrum and frequencies. However, high frequency reuse factor can cause potential cochannel interference or an increase in carrier-to-interference power ratio (CIR or C/I). IMMARSAT has reported that a reuse factor of 5–30 is possible with multiple spot beams employed by commercial HTS. Depending on the number of beams implemented on-board of the satellite, the cost for HTS can be twice of the cost for a regular satellite. But, the cost per bit for HTS is much lower than the regular satellite. HTS is a preferred option for point-to-point services, for example, beyond line-of-sight (BLOS) cellular phone services. **Table 1** provides a summary of the comparison of HTS and regular commercial satellites [2].

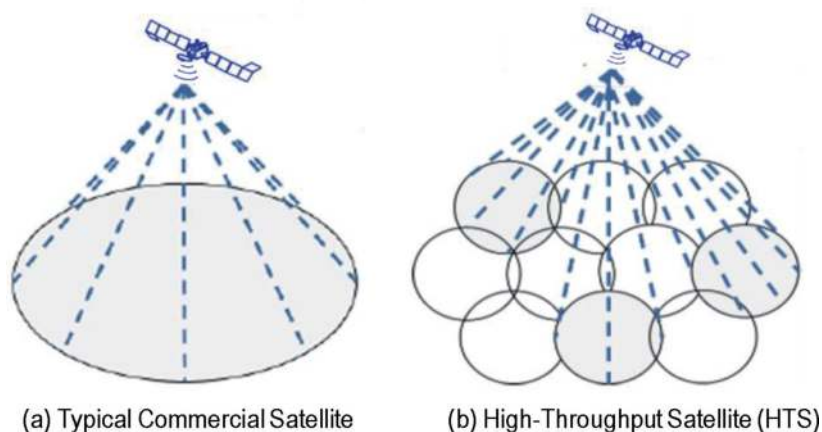


Figure 1.
Typical commercial satellites and HTS configurations.

Comparison factor	Typical regular commercial satellite	Typical high-throughput satellite (HTS)	Remark
Operational frequency band	C-band, Ku-band, Ka-band	Ku-band, Ka-band	It should be noted that for data presented here, all satellites and supply are not equal; various technical, regulatory, and commercial parameters come into play when comparing the two-type satellites. Data collected from IMMARSAT. Source: see [2]
Throughput capability (Gbps)	~1-10	~5-300+ (with frequency reuse in multiple spot beam)	
Typical cost including launch (USD)	~200-300	~300-500 (cost can be twice of regular satellite)	
Advantages	Wide coverage; preferred solution for point-to-multipoint communication	Higher bandwidth/ lower cost per bit; preferred option for point-to-point services	
Disadvantages	Limited supply available; lower spectrum efficiency for an equivalent frequency	Higher upfront costs; difficult to find enough customers to fill each of the beams	

Table 1.
 Comparison of typical commercial satellites and HTS.

3. Typical commercial satellite network topologies

This section describes the most commonly used satellite network topologies, namely “Star” satellite network (Section 3.1) and “Mesh” satellite network (Section 3.2).

3.1 Typical “star” satellite network

A typical commercial satellite network topology consists of an uplink from a central anchor station (aka satellite Gateway or satellite Hub) to a satellite and a downlink from the satellite to users. Users can be mobile or fixed users. Mobile users can be located in an airplane, a boat, or a car. Fixed users can be located in a building or a cellular base station. The “star” satellite network is derived from a spoke-hub distribution paradigm in computer networks, where one central hub serves as a conduit to transmit messages among network users [3]. Thus, for star satellite networks, all communications will be passed through a satellite gateway. As shown in **Figure 2**, if Mobile User 1 wants to talk to Mobile User 2, Mobile User 1 needs to send its messages to the satellite gateway (yellow lines), and satellite gateway relays that messages to Mobile User 2 (red lines).

3.2 Typical “mesh” satellite network

The “mesh” satellite network topology is derived from a local network topology, where the network nodes are connected to each other directly, dynamically, and nonhierarchically to as many other nodes as possible [4]. In this network topology, the network nodes can cooperate with one another to route data from one user to another user efficiently. Hence, for mesh satellite network, Mobile User 1 can talk to fixed user directly without going through the satellite gateway (solid lines), and Mobile User 2 can also talk to the fixed user directly (dash lines).

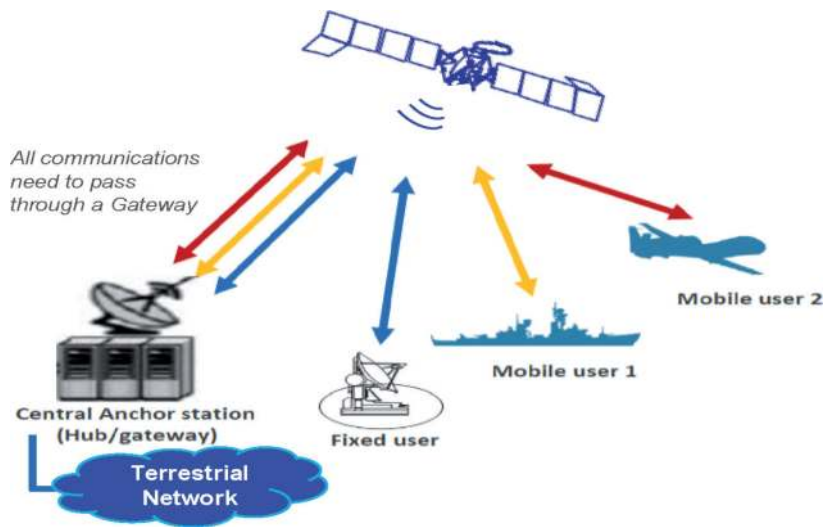


Figure 2.
Typical “star” satellite network.

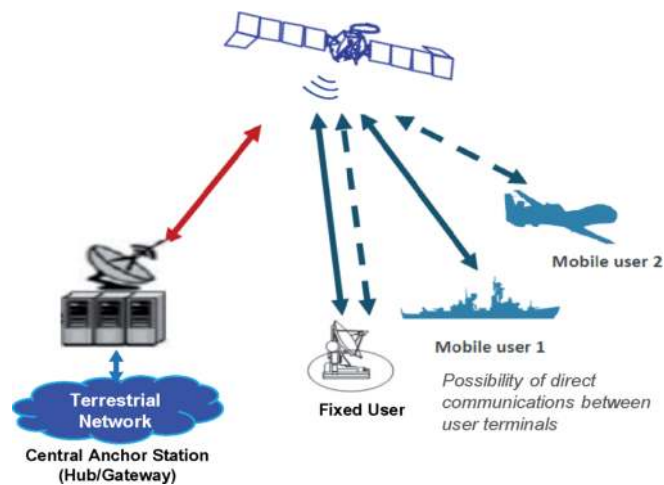


Figure 3.
Typical “mesh” satellite network.

Any one of the user within the network can send the messages to a terrestrial network through the red lines representing uplink and downlink between the satellite gateway and the satellite (**Figure 3**).

Star satellite network topology does not require advanced satellite payload processing on-board and multiple beam, but mesh satellite network requires advanced on-board processing and multiple beam allowing one user to communicate to another user automatically and effectively. Section 4 discusses various satellite payload architectures used in regular satellite and HTS for star and mesh satellite network applications.

4. Legacy, existing, and advanced satellite payload architectures

This section presents an overview of legacy, existing, and advanced satellite payload architectures. Section 4.1 presents legacy ABPS payload architecture, Section 4.2 provides a description of a typical existing DBPS payload architecture,

Section 4.3 discusses AdDBPS-DCB payload architecture, and Section 4.4 provides an overview of AR-OBPS payload architecture.

4.1 Legacy analog bent-pipe satellite (ABPS) payload architecture

A typical legacy ABPS payload architecture is depicted in **Figure 4**, where the payload has multiple beam antennas (MBAs) using parabolic dishes. For this architecture, the RF signal is received at the satellite payload and amplifies by a low noise amplifier (LNA) for increased received signal-to-noise power ratio (SNR). The RF signal with increased SNR is downconverted (D/C) to an intermediate frequency (IF) and processed by an IF filter to clean up the signal from adjacent interference and out-of-band noise. The clean-up signal is then (a) routed to the proper downlink port by an IF analog switching circuit and upconverted (U/C) to RF, (b) combined by a multiplexer (MUX), and (c) amplified by a high-power amplifier (HPA) for downlink transmission.

As illustrated in **Figure 5**, there are two options for the D/C, namely Option 1 (see **Figure 5(a)**) is a double downconverter using two local oscillators (LOs) to downconvert RF signal to IF signal with stable and low phase noise, and Option 2 (see **Figure 5(b)**) is single downconverter using a LO downconverting RF signal directly to an IF signal. Option 1 is being used in many legacy, existing, and advanced satellite payloads. Option 2 is mostly used in advanced satellite payloads.

Figure 5(c) shows commercial-of-the-shelf (COTS) phase noise characteristics for typical LOs operating at X-band, Ku-band, and Ka-band. X-band, Ku-band, and Ka-band illustrated in this figure correspond to 7–11.2, 12–18, and 26.5–40 GHz, respectively. The main advantages of Option 2 using single downconversion are its low cost, small size, and low power consumption (also known as small SWAP-C). This option uses the smallest number of external components as compared to Option 1 using double downconversion, which is also known as super heterodyne receiver [5]. However, Option 2 suffers amplitude and phase imbalances caused by imperfect references associated with I-Q components, direct current (DC) signal due to self-mixing, and flicker noise.¹ Option 1 does not suffer from these problems and offers excellent selectivity and sensitivity, that is, better rejection of adjacent interferences. Option 1's disadvantages are the integration complexity and high SWAP-C.

In satellite electronic communications, MUX is a multiplexer, which is a device that selects several (multiple) analog (or digital) input signals and outputs a single signal. **Figure 6(a)** describes a functional MUX (aka multiplexer) circuit. On the contrary, **Figure 6(b)** depicts a DEMUX (aka demultiplexer), which is an electronic device that sends a single input signal to multiple signal outputs.

4.2 Existing digital bent-pipe satellite (DBPS) payload architecture

Figure 7 presents an existing DBPS payload architecture using on-board digital channelizer. Similar to analog payload, there are two options for the RF-to-IF down-conversion process. Double-downconversion process is typically used for digital bent-pipe payload architecture.

Figure 8 depicts typical RF-to-IF (or baseband) downconversion and digitization and sampling processes for a commercial DBPS payload architecture. The RF-to-IF process shown in this figure uses Option 1, double downconversion, and the digitization and sampling process employing bandpass sampling with

¹ Flicker noise is a type of electronic noise with a $1/\text{frequency}$ power spectral density.

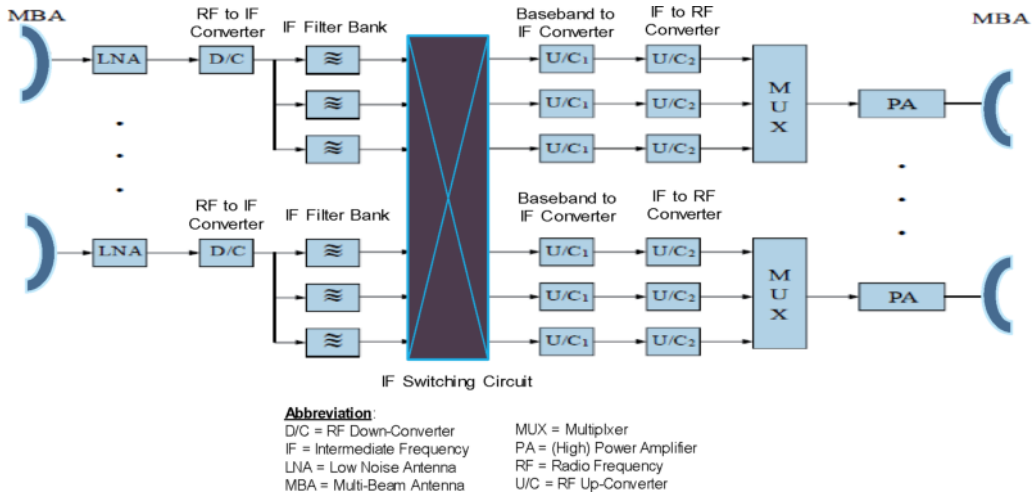


Figure 4. Legacy ABPS payload architecture.

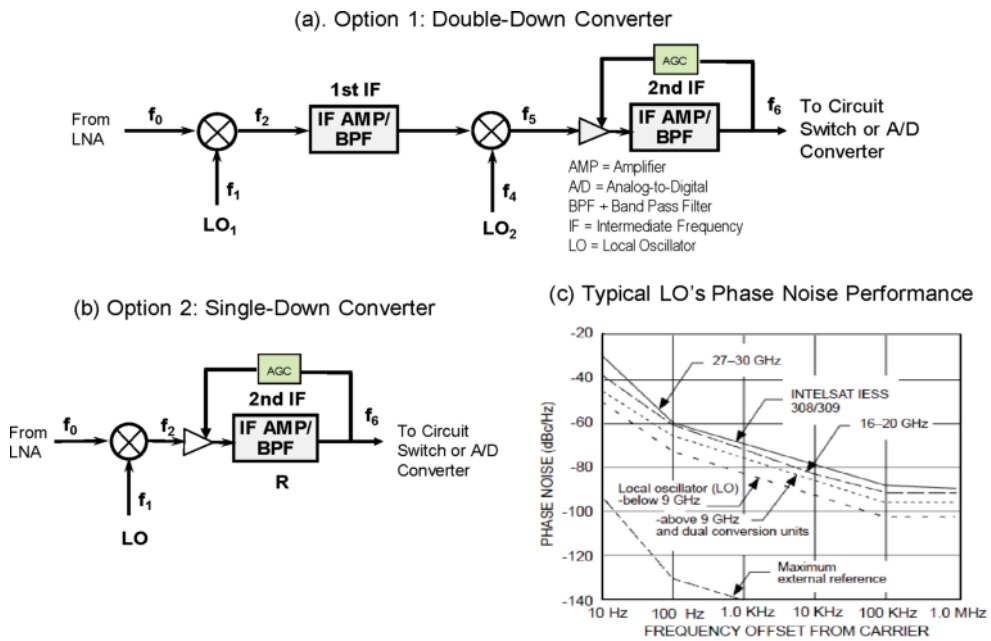


Figure 5. Options for RF downconversion and associated LO's phase noise.

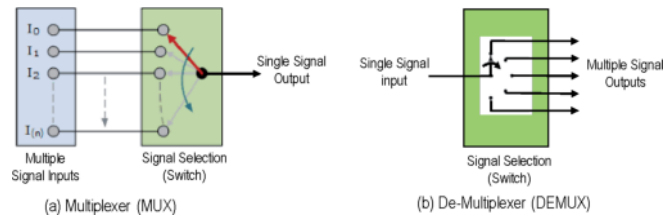


Figure 6. Functional block diagrams of MUX and DEMUX.

digital quadrature technology [6]. The RF bandwidth (BW) associated with the RF bandpass filter (BPF) is selected to match with an over channel bandwidth (e.g., a maximum of 500 MHz for Ku-band). The automated gain control (AGC)

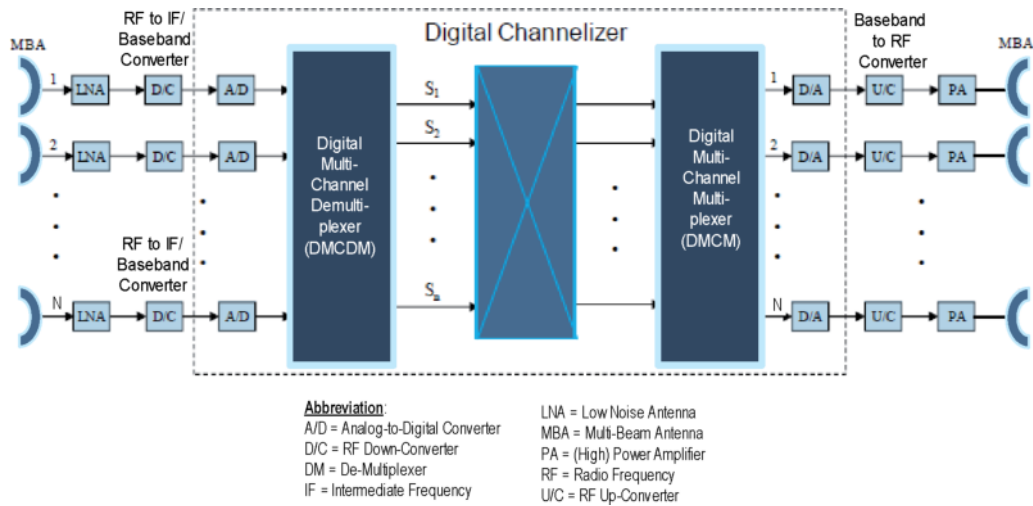


Figure 7.
 Existing DBPS payload architecture.

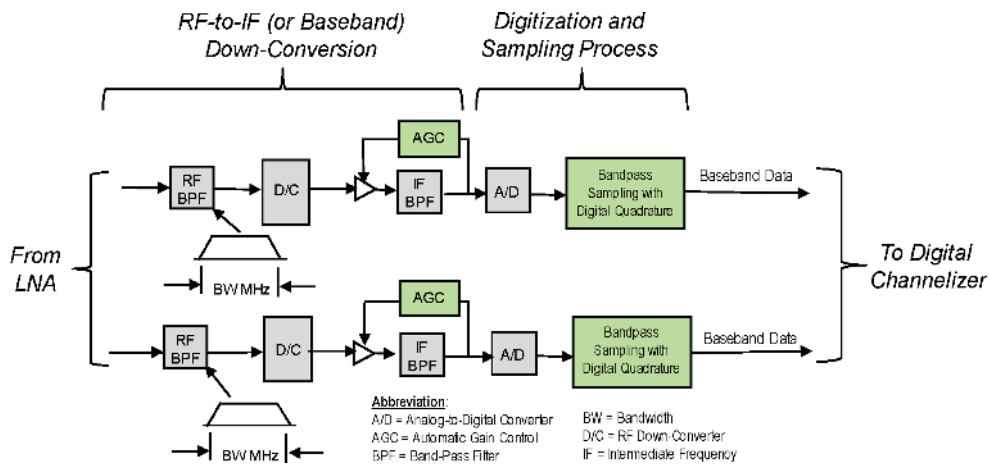


Figure 8.
 Typical R/F downconversion and digitization processing approach.

is designed to maintain a constant power over the specified channel bandwidth. There are several advantages associated with bandpass sampling with digital quadrature techniques, including (a) no phase and amplitude imbalances; (b) digital finite impulse response (FIR) filters are flexible and computational complexity with linear phase introducing a constant group delay; (c) only one A/D converter is required (less weight and power); and (d) when the sampling period is set at one-quarter of the carrier frequency, the reference in-phase and quadrature components reduce to an alternating sequence between I-channel and Q-channel [6].

As shown in **Figure 9**, the key design issue associated with the digitization and sampling processing is the selection of required number of bits of the analog-to-digital (A/D) conversion to (1) achieve optimum loading factor (LF) and (2) minimize the quantization noise. The LF is defined as the root mean square (RMS) of the total input signal voltage-to-A/D converter saturation voltage ratio. The total input signal voltage includes desired signal voltage (S) plus noise voltage (N) plus interference voltage (I). **Figure 10** illustrates an optimum LF as a function of number of bit of a typical A/D converter. As an example, for 4-bit,

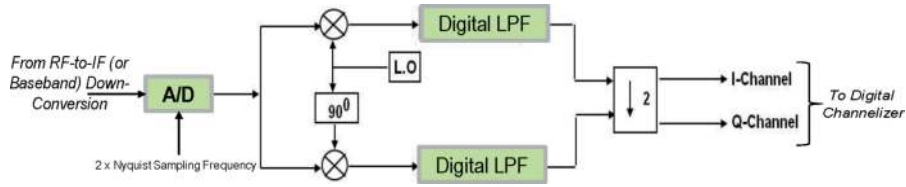


Figure 9. Existing digitization and sampling processing using bandpass sampling with digital quadrature technique.

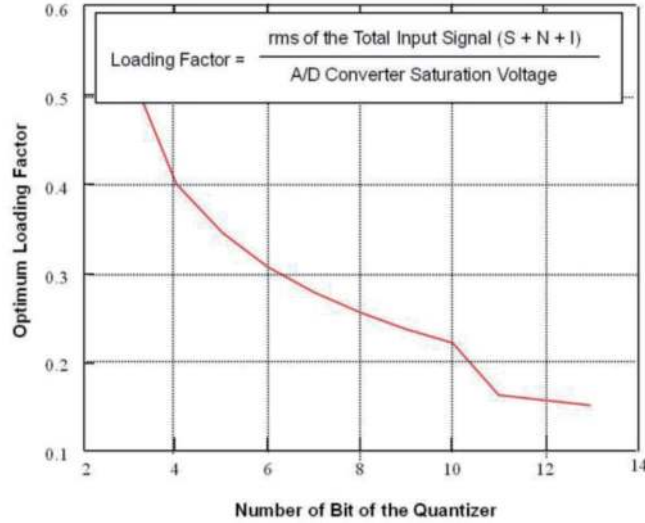


Figure 10. Optimum LF as a function of number of bit of A/D converter.

the optimum LF is about 0.4. In conjunction with LF, the number of bit should be selected to maximize the signal-to-quantization noise ratio (SQNR) using the following relationship:²

$$SQNR \approx 1.761 + 6.02.N \text{ dB} \tag{1}$$

As an example, when $N = 4$ bits, signal-to-quantization noise ratio is about 25.84 dB.

The key feature of DBPS payloads is the flexibility of the digital channelizer. Current digital technologies allow for the implementation of robust and reconfigurable digital channelizer adapting to require the number of users and associated users' data rates. A typical flexible digital channelizer using polyphase/discrete Fourier transform (DFT) technology is shown in **Figure 11**.

As shown in **Figure 11**, the heart of a typical digital channelizer is a polyphase-filter network (or simply a polyphase network) and a DFT processor. A typical polyphase network with a DFT processor is described in **Figure 12**. The polyphase network consists of a set of N_C digital filters with transfer function $H_0, H_1, \dots, H_{N_C-1}$, which is obtained by shifting a basic low pass complex filter function along the frequency axis [7]. As an example, for a typical 500 MHz channel bandwidth, assuming for a typical user data rate of 4 MHz and a guardband of 1 MHz, digital channelizer, $N_C = 500/(4 + 1) = 100$, that is, the number of filter is 100, and each has a total of 5 MHz bandwidth. A change in sampling frequency by a factor of N_C can

² Quantization (signal processing). Available from: [https://en.wikipedia.org/wiki/Quantization_\(signal_processing\)](https://en.wikipedia.org/wiki/Quantization_(signal_processing)).

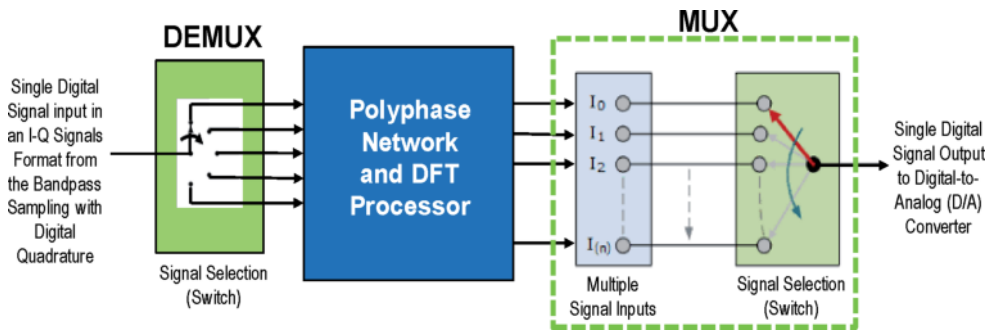


Figure 11.
 Typical digital channelizer using polyphase/DFT technology.

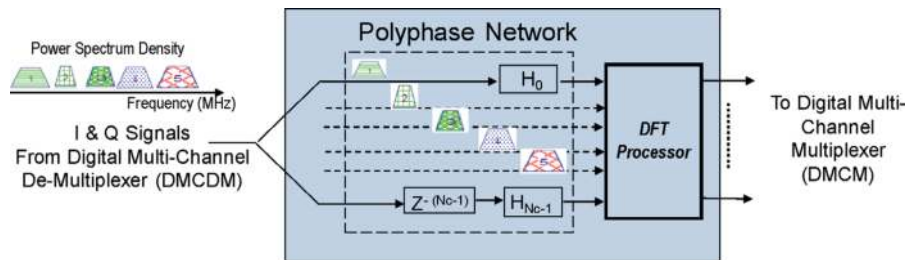


Figure 12.
 Typical Polyphase/DFT Technology.

be introduced, thus allowing the circuit in different paths of the polyphase network to operate at lower frequency than the original sampling frequency. A practical implementation of a high-throughput low-latency polyphase channelizer can be found in [8, 9].

Figure 12 shows an example of five input signals, namely S_1 , S_2 , S_3 , S_4 , and S_5 , and the channelizer will select signal interest by filtering out the other signals. As an example, the signal line with the filter transfer function of H_0 filters out S_2 , S_3 , S_4 , and S_5 and sends S_1 as an output signal.

4.3 Advanced digital bent-pipe satellite using digital channelizer and beamformer (AdDBPS-DCB) payload architecture

For a typical commercial HTS system architecture, it usually requires on-board multiple beam phase array (PA) antenna with associated adaptive digital beam-former network (DBF) for spot beamforming and frequency reusing of the spot beams when the beams are not located near each other. **Figure 13** describes a typical AdDBPS-DCB payload architecture, where the digital channelizer is combined with a DBF to make a “digital channelizer and beamformer” (DCB) [10–12]. For this payload architecture, the key feature that differentiates this architecture with the ones discussed above is the combined digital channelizer using polyphase network/DFT processor and DBF (PolyN/DFT-DBF).

As pointed out in [10–12], DCB architecture shown in **Figure 13** can be designed to (1) form individual beams for each active receive and transmit communication channels; (2) adaptively generate channel beam steering weights to dynamically vary the bandwidth, location, and shape of each beam based on traffic demands and the locations of other, potentially interfering beams avoiding adjacent channel interference; (3) use digital beamforming weight calibration to compensate for the temporal and thermal phase and amplitude response variations inherent in analog multibeam phased array antennas; and (4) adjust the gain of individual

receive-and-transmit channel beams automatically to compensate for propagation path and analog payload response variations. In general, there are two possible DCB implementation approaches, namely DCB Approach 1 and DCB Approach 2 [13].

Figure 14 describes the DCB Approach 1 for processing the uplink signals, where the uplink signals are individually processed by the digital channelizer (i.e., PolyN/DFT processing) and DBF independently and separately. DCB Approach 1 requires a larger computational load because each DBF processes all the user link bandwidth (e.g., $S_1, S_2, S_3, S_4,$ and S_5 in **Figure 12**) at all times to form multiple beams.

DCB Approach 2 is shown in **Figure 15**, where DCB utilizes an unified processing approach with each DBF processes only the bandwidth corresponding to a beam (S_1 in **Figure 12**) at normal times. During anomaly operation condition (e.g., natural disaster event), when the bandwidth has to be reassigned to specific areas, the arithmetic load on DBF can be reduced by implementing multiple DBFs, with each capable of processing a bandwidth narrower than that assigned to a beam (i.e., smaller channel unit). This approach enables a reduction in wasteful arithmetic resource usage on bandwidth.

If one defines the number of multipliers, D implemented in each Tx/Rx DBF as C/fop , where C is the computational load of a DBF (multiplications/sec), and fop is the operation frequency of the multiplier. Let us compare D calculations between DCB Approach 1 and DCB Approach 2. Let us assume the following parameters: n is the number of array elements, m is the number of beams, an userlink processing bandwidth of 28 MHz, 5 frequency repetitions of the userlink, and an operating

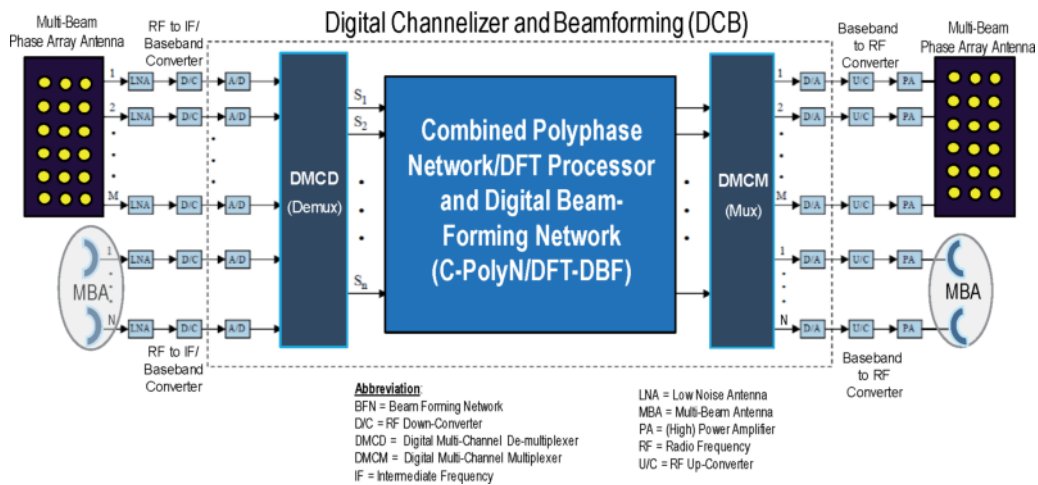


Figure 13.
AdDBPS-DCB payload architecture.

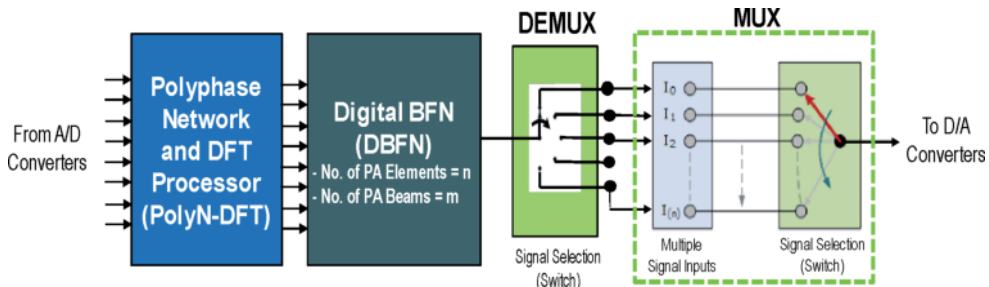


Figure 14.
DCB Approach 1: PolyN/DFT and DBFN individual processing.

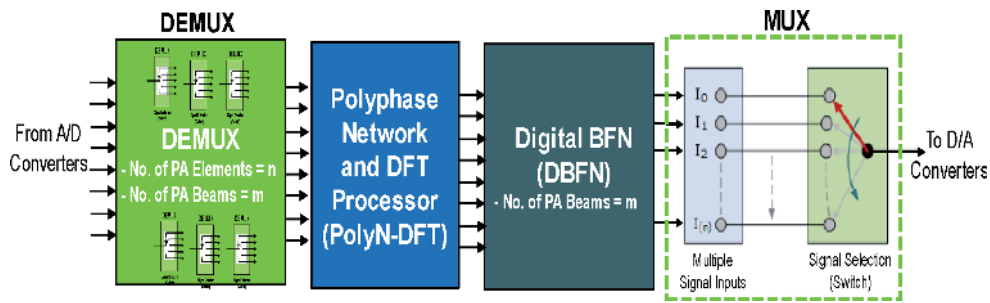


Figure 15.
 DCB Approach 2: Unified and combined PolyN/DFT and DBFN individual processing.

frequency of multiplier of 256 MHz. Using these values, D for the DBF/channelizer of the DCB Approach 1 configuration becomes [13]:

$$\frac{(n \times 4 \times m \times 28 * 106 [\text{multiplications / s}])}{(256 * 106 [\text{multiplications / s}])} \quad (2)$$

and that for DCB Approach 2 configuration becomes [13]:

$$\frac{(n \times 4 \times m \times 28 * 106 / 5 [\text{multiplications / s}])}{\left(256 * 106 \left[\frac{\text{multiplications}}{s} \right] \right) \times 2} \quad (3)$$

The latter calculation assumes an ideal case in which DBF network (DFBN) processing is performed on a channel-by-channel basis. The complexity of DCB Approach 2 configuration is 10 times less complex than DCB Approach 1.

As pointed out in [12], the DBFN when coupled with a digital channelizer (aka DCB) offered more capabilities with many advantages. Nguyen et al. [14] developed a computer simulation model of a typical DBFN in MATLAB and presented simulation results for X, Ku, and Ka BFNs using 60-element, 104-element, and 149-element, respectively. **Figure 16** is an extracted Ka-band BFN result showing the achievable antenna gain of 45.5 dB at 3-dB beamwidth of 0.9°. For practical applications, the DBFN will shape the beam size depending on the coverage area and desired number of beams. Nguyen et al. [14] pointed out that for 2.5° coverage area and the desired number of beams of 7, the minimum 3-dB beamwidth of 1.1° is required. Nguyen et al. [14] also pointed out that DCB can provide a significant increase in frequency reuse, where the frequency reuse is defined as the number of times a satellite can reuse the same spectrum and frequencies. High frequency reuse factor can cause potential cochannel interference (CCI) that results in a decrease in carrier-to-interference power ratio [aka (C/I) CCI]. As pointed out in [14], for dynamic allocation using real-time allocation of beams so that the coverage radius of a cell is equal to the satellite pointing error, assuming satellite pointing error of 0.02 degree pointing error, the (C/I)CCI is about 25 dB for frequency reuse factor 40 [14].

4.4 Future advanced regenerative on-board processing satellite (AR-OBPS) payload architecture

Figure 17 depicts a potential future AR-OBPS payload architecture [10]. The payload includes (1) a typically set of digitized analog multiple beam antenna (MBA) input signals, digitally frequency division demultiplex each input signal to produce single carrier per channel (SCPC) signal data and demodulate and decode

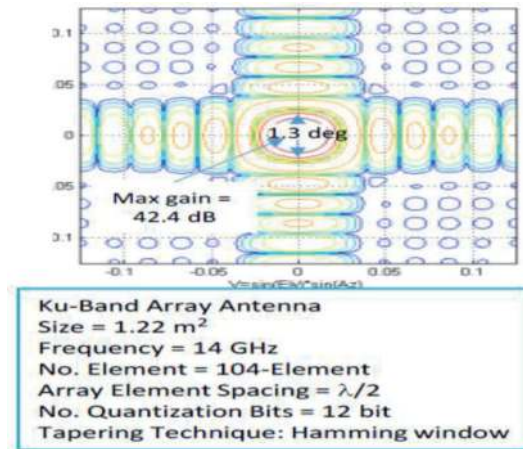


Figure 16. Antenna beamwidth and gain of a notional Ka-band DBFN with 12-bit quantization [14].

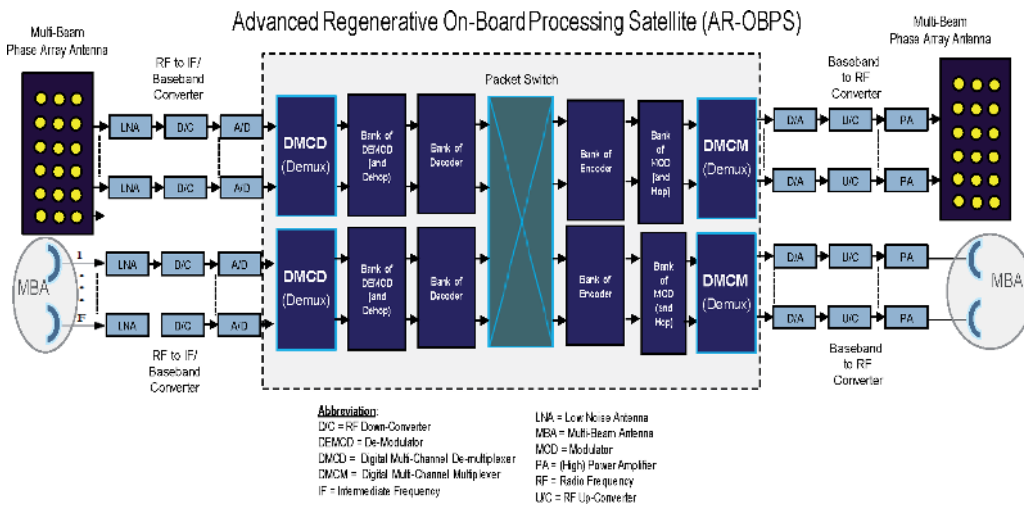


Figure 17. AR-OBPS payload architecture.

individual traffic channels to recover the original information bits transmitted on the uplink; (2) a set of digitized analog multibeam phase array antenna (MB-PAA) input signals, digitally frequency division demultiplex each input signal to produce SCPC signal data and demodulate and decode individual traffic channels to recover the original information bits transmitted on the uplink; and (3) fast packet switches are typically employed at the AR-OBPS payload's core to realize statistical multiplexing gains by efficiently packing and moving data through the switch and onto the downlink in bursty uplink transmission applications. Moreover, the digital bandwidth (in Hz) through the AR-OBPS switch is at least 25 times less³ than that supported by an equivalent (pre-demodulation) digital baseband switch at the center of a DC- or DCB-based system. AR-OBPS payload can also support digital beamforming, following the frequency division demultiplexing operation, if a phased array is employed in place of the analog MBA. On the secondary (output) side of the switch, each user's binary information is channel encoded and modulated onto a carrier. The modulated carrier data thus produced are multiplexed,

³ Assumes 1 bps/Hz modulation efficiency, 10 bit signal data quantization, and 2.5× practical Nyquist sampling rate.

digital-to-analog converted, and passed through an analog reconstruction filter to generate output signals for the transmit portion of the communication payload. The channel codes and modulations employed on the uplink (input) communication channels clearly do not need to be the same as the channel codes and modulations used on the transmitted downlink channels. Hence, an AR-OBPS payload can serve as a “translator” facilitating single-hop communications between terminals employing different link protocols. However, if either the digital multichannel demultiplexer (DMCD), demodulator, decoder, or digital multichannel multiplexer (DMCM) encoder modulator, multiplexer (MCEM2) functions are implemented in ASICs to minimize size-weight-and-power (SWaP), then the AR-OBPS system becomes somewhat inflexible, unable to support either uplink or downlink terminals, respectively, using communication protocols differing from those for which the AR-OBPS was specifically designed. For this reason, AR-OBPS systems are typically employed in support of “private networks” in which the communication satellite service provider only accommodates terminals designed to work on the provider’s network. Iridium and Spaceway are two examples of commercial AR-OBPS-based communication satellite systems.

5. Satellite system architectures for 5G cellular phone applications

Sections 5.1 and 5.2 present a notional satellite system architecture using AdBPS-DCBS satellite payload and AR-OBPS satellite system architecture for 5G cellular phone applications, respectively.

5.1 AdBPS-DCBS satellite system architecture for 5G applications

AdBPS-DCBS satellite payload can be used to support 5G users. There are potentially two satellite system architecture options for using AdBPS-DCBS satellite payload to support 5G mobile user equipment (aka 5G-UE), namely AdBPS-DCBS Option 1 and AdBPS-DCBS Option 2. For AdBPS-DCBS Option 1, the AdBPS-DCBS satellite provides communication services directly to 5G-UEs. While in AdBPS-DCBS Option 2, the satellite provides services to 5G-UEs through the 5G relay nodes (RNs). **Figure 18** illustrates the AdBPS-DCBS satellite system architecture for (a) AdBPS-DCBS Option 1 and (b) AdBPS-DCBS Option 2 [15].

Figure 18(a) shows that the AdBPS-DCBS satellite requires new radio (NR) interfaces between (1) AdBPS-DCBS satellite and terrestrial gateway (GW) and (2) AdBPS-DCBS satellite and 5G-UEs. In addition, it is also required a 5G narrow-band (gNB) processing station to process the 5G signals from the next generation core (NGC) network before passing the 5G data to public data network.

5.2 AR-OBPS satellite system architecture for 5G applications

Similar to AdBPS-DCBS satellite payload, AR-OBPS satellite payload can also be used to support 5G users. There are also two satellite system architecture options for using AR-OBPS payload to support 5G mobile user equipment, namely AR-OBPS Option 1 and AR-OBPS Option 2. For AR-OBPS Option 1, the AR-OBPS satellite provides communication services directly to 5G-UEs. For AR-OBPS Option 2, the satellite provides services to 5G-UEs through the 5G RNs. **Figure 19** describes these two AR-OBPS architecture options, namely (a) for AR-OBPS Option 1 and (b) for AR-OBPS Option 2. For these two system architecture options, the gNB processing is now incorporated into the AR-OBPS satellite payload and no longer required for the ground system. The GW now can pass the 5G data directly to the NGC. The

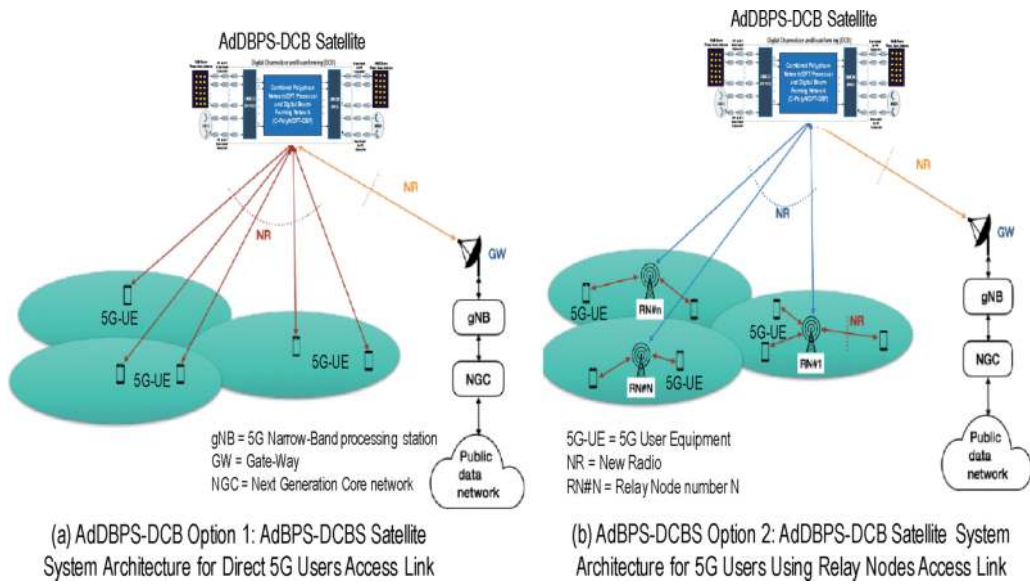


Figure 18.
AdDBPS-DCB satellite system architectures for supporting 5G users.

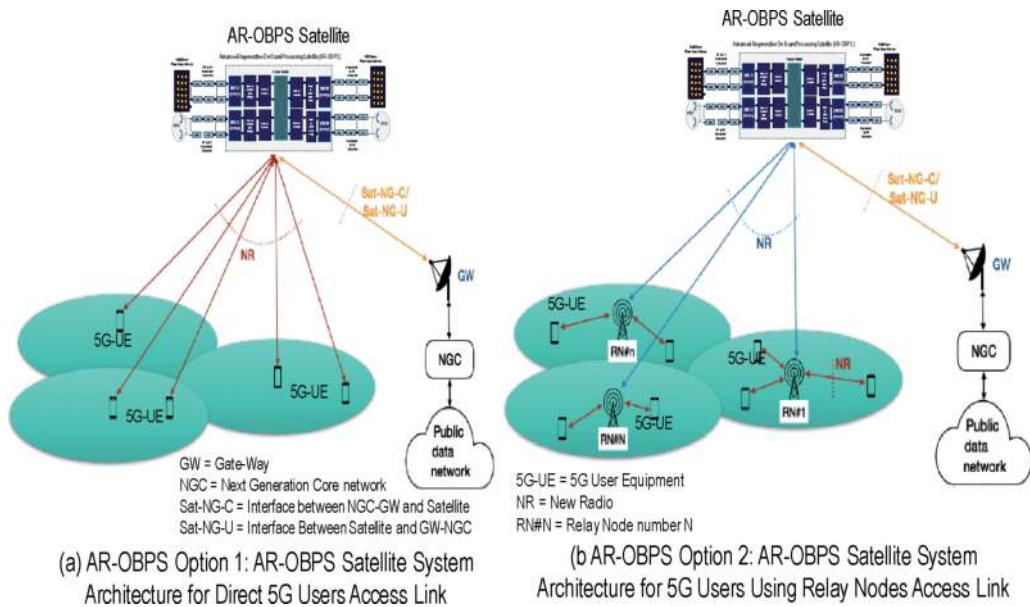


Figure 19.
AR-OBPS satellite system architectures for supporting 5G users.

decoding-demodulation and encoding-modulation processing on-board of the satellite will be designed to align with the 5G waveform specifications, including 5G modulation and coding schemes.

Figure 19(a) shows that the AR-OBPS satellite also requires NR interfaces between (1) AR-OBPS satellite and GW and (2) AR-OBPS satellite and 5G-UEs. Similar to AdBPS-DCBS satellite system architecture options, the NR interfaces between the AR-OBPS satellite and 5G-UEs are new. Since the gNB processing is now placed at AR-OBPS satellite payload, the NR interfaces between AR-OBPS satellite and 5G-UEs are not the same as the AdBPS-DCBS satellite and 5G-UEs. To show the differences between the two, **Figures 19(a)** and **(b)** use Sat-NG-C and Sat-NG-U to indicate the new radio interface between (1) terrestrial GW-NGC-and-AR-OBPS satellite and (2) AR-OBPS satellite-and-terrestrial GW-NGC, respectively.

6. Conclusion

This chapter uses a top-down approach for providing an overview of legacy, existing, and future advanced satellite payload architectures for future wireless communication applications. The chapter focuses on the commercial satellite technologies based on the research results presented in [1, 2]. Section 2 provides the comparison results performed by Inmarsat describing the technical characteristics and associated advantages and disadvantages between commercial HTS and typical satellite systems currently available in commercial satellite market. In Section 3, two most commonly satellite network topologies used by existing commercial satellite networks are presented, and the concept of satellite uplink and downlink associated with star satellite network and mesh satellite network is discussed. The satellite network topologies presented lead to Section 4, where four satellite payload architectures are discussed. The legacy analog ABPS payload architecture is shown to be more appropriate for star satellite network than mesh network. Existing digital DBPS and AdDBPS-DCB payload architectures are designed for supporting mesh satellite network with large number of mobile users. Future advanced digital satellite payload architecture, namely AdDBPS-DCB, is also presented in this section. With decoding-demodulating and encoding-modulating processing on-board of the satellite, AR-OBPS allows for packet switching on-board and higher quality of service (QoS) than existing DBPS and AdDBPS-DCB at the expense of higher SWAP-Cost (SWAP-C). Section 4 of the chapter discusses the applications of AdBPS-DCBS and AR-OBPS payloads for supporting 5G users. Four satellite system architecture options are presented for supporting the future 5G users.

Conflict of interest

The preparation of this chapter was not funded by Gulfstream, and it was done by the author using his own time and resources; thus, it does not represent the Gulfstream's view on the results presented in this chapter.

Notes/Thanks/Other declarations


The author wishes to thank his wife, Annie Luu-Nguyen, for her immense patience and support.

Author details

John Nguyen
JohnDTN Consulting Services, Huntington Beach, California, USA

*Address all correspondence to: johndncva@gmail.com

IntechOpen

© 2020 The Author(s). Licensee IntechOpen. This chapter is distributed under the terms of the Creative Commons Attribution License (<http://creativecommons.org/licenses/by/3.0>), which permits unrestricted use, distribution, and reproduction in any medium, provided the original work is properly cited. 

References

- [1] Magnuson S. Commercial space—Not military—Driving satellite innovation. *National Defense Magazine*. 2018. Available from: <https://www.nationaldefensemagazine.org/articles/2018/4/17/commercial-space-not-military-driving-satellite-innovation>
- [2] Revillon P. Fundamentals and Dynamics of the Satellite Communications Business. Presented at the Euroconsult for Inmarsat Capital Markets Day in 2016. Available from: www.euroconsult-ec.com
- [3] Star Network. Wikipedia. Available from: https://en.wikipedia.org/wiki/Star_network
- [4] Mesh Network. Wikipedia. Available from: https://en.wikipedia.org/wiki/Mesh_networking
- [5] Superheterodyne Receiver. Wikipedia. Available from: https://en.wikipedia.org/wiki/Superheterodyne_receiver
- [6] Sadr R, Shahshahani M. On Sampling Band-Pass Signals, TDA Progress Report 42-96. Pasadena, California: NASA-Jet Propulsion Laboratory; 1988
- [7] van der Veldt K, van Nieuwpoort R, Varbanescu AL, Jesshope C. A polyphase filter for GPUs and multi-core processors. In: *Proceedings of the Workshop on High-Performance Computing for Astronomy*; Delft, Netherlands; 18 June, 2012. pp. 33-40
- [8] Kim SC, Bhattacharyya SS. Implementation of a high-throughput low-latency polyphase channelizer on GPUs. In: *EURASIP Journal on Advances in Signal Processing*; 2014. Available from: <http://asp.eurasipjournals.com/content/2014/1/141>
- [9] Ejima F, Akita M, Fujimura A. Digital Channelizer for High Throughput Satellite Communications, Technical Paper. Mitsubishi Electric Advance (Technical Journal published by Mitsubishi); 2014. pp. 7-10
- [10] Butash TC, Marshall JR. Leveraging digital on-board processing to increase communications satellite flexibility and effective capacity. In: *28th AIAA ICSSC*. AIAA 2010-8715; Anaheim, CA; 30 August–2 September 2010
- [11] Sichi SF, Ziegler HE. Beamforming architectures for advanced MSS network deployment. In: *29th AIAA ICSSC*; AIAA 2011-8021; Nara, Japan; 28 November–01 December, 2011
- [12] Freedman JB, Marshack DS, et al. Advantages and capabilities of a beamforming satellite with a space-based digital processor. In: *32nd AIAA International Communications Satellite Systems Conference (ICSSC)*; AIAA 2014-4321; San Diego, CA; 4-7 August 2014
- [13] Komiyama N, Miura A, Orikasa T, Fujino Y. Development of resource allocation re-construction technology (digital beam former and digital channelizer). *Journal of the National Institute of Information and Communications Technology*. 2015. pp. 151-163
- [14] Nguyen TM, Guillen A, Matsunaga S. Practical achievable capacity for advanced SATCOM on-the-move. In: *2016 IEEE MILCOM Conference Proceedings*; 2016
- [15] Guidotti A, Vanelli-Coralli A, Conti M, Andrenacci S, Chatzinotas S, Maturo N, et al. Architectures and key technical challenges for 5G systems incorporating satellites. *IEEE Transactions on Vehicular Technology*. 2019. pp. 2624-2639